TRIUMF — RESEARCH PROPOSAL	Experiment no.	Sheet 1 of 17

Title of proposed experiment:

A study of the partial and total cross sections of the ^{8}Li(α,n)^{11}B reaction at astrophysically relevant energies.

Name of group: Rstart

Spokesperson for group: P. Walden/A. M. Laird

E-Mail address: mrspi@triumf.ca Fax number: 604-222-1074

Members of the group (name, institution, status, per cent of time devoted to experiment)

P. Walden	TRIUMF	Senior Research Scientist	30%
R. Boyd	Ohio State University	Professor	20%
L. Buchmann	TRIUMF	Senior Research Scientist	20%
A. A. Chen	McMaster University/TRIUMF	Assistant Professor	10%
J. D'Auria	Simon Fraser University	Professor	20%
B. Fulton	University of York	Professor	10%
U. Greife	Colorado School of Mines	Assistant Professor	10%
D. Hutcheon	TRIUMF/University of Alberta	Senior Research Scientist	10%
A. M. Laird	TRIUMF	Research Associate	30%
Z. Li	CIAE	Research Associate	50%
A. Murphy	University of Edinburgh	Lecturer	20%
S. Nishimura	RIKEN	Faculty	10%
S. Park	TRIUMF	Research Associate	40%
D. Reitzner	Ohio State University	Research Associate	20%
J. Rogers	TRIUMF	Senior Research Scientist	10%
F. Sarazin	TRIUMF	Research Associate	10%
A.C. Shotter	TRIUMF	Professor	10%

Start of preparations:	now
Date ready:	Fall 2004
Completion date:	2006

Beam time requested:

12-hr shifts	Beam line/channel	Polarized primary beam?
20 (^{8}Li)	ISAC-HE/TUDA	no
20 (^{9}Be)	OLIS	no
10 (^{7}Li)	OLIS	no

We propose to measure the total cross section of the ^{8}Li(α,n)^{11}B reaction as well as the partial cross sections for the population of excited states in ^{11}B. This reaction rate is important for predictions of light element abundances from inhomogeneous big bang (IBB) models and also plays a role in r-process nucleosynthesis in core collapse supernovae scenarios. Previous measurements have produced inconsistent results and have been unable to study the lowest resonances of interest.

The proposed experimental setup consists of a specially designed cylindrically symmetric ion chamber surrounded by an array of γ-ray detectors. The ion chamber tracks only scattered particles and reaction products due to its cylindrical symmetry. ^{11}B from the ^{8}Li(α,n)^{11}B reaction are tracked and identified in the detector and any coincident γ-rays corresponding to the decay of excited states in ^{11}B are measured. From these data, angular distributions and total cross sections for the states populated can be determined.

Experimental area

ISAC-HE, TUDA

Primary beam and target (energy, energy spread, intensity, pulse characteristics, emittance)

p (500MeV, 40μA)
ISAC production target (Ta)

Secondary channel ISAC-HE/TUDA

Secondary beam (particle type, momentum range, momentum bite, solid angle, spot size, emmittance, intensity, beam purity, target, special characteristics)

10^7 pps ^{8}Li (unstable), 0.15 - 1.2 MeV/u
10^7 pps ^{9}Be (stable), 0.7 - 1.5 MeV/u
10^7 pps ^{7}Li (stable), 0.15 - 1.2 MeV/u

TRIUMF SUPPORT:

TUDA services as presented to and reviewed by TRIUMF. This includes an electronics cabin and special grounding.
Operational support and data acquisition support.

NON-TRIUMF SUPPORT

The TUDA facility, including considerable manpower for setup and operation, is provided by the University of Edinburgh, University of York, RIKEN and the Ohio State University groups. A NSERC project grant for manpower and equipment development has been submitted. This grant will fund the development and construction of the ion chamber and related equipment, including the gas handling system, diagnostics box and electronics. The BGO array and related electronics will be provided by the DRAGON collaboration.

Standard TUDA operation with short lived radioactive isotopes, (^{8}Li). Low voltage detectors and electronics. Gas filled detector. Isobutane.

1 Scientific Justification

1.1 Big Bang Nucleosynthesis

The now well-established tension between theoretical prediction and observation of the primordial light element abundances[1] has spawned some interest in nonstandard models of big bang nucleosynthesis. One of the most interesting modifications to the standard model (SBBN) is relaxation of the assumed density uniformity at the time of big bang nucleosynthesis, resulting in the inhomogeneous big bang models of nucleosynthesis (IBBN). Although the recent cosmic microwave background measurements strongly suggest that the baryonic density determined by the SBBN is very close to the correct value, the robustness of the Big Bang models is an important issue that must be addressed. Thus the predictions of the IBBN model are important in determining the uniqueness of the Big Bang model.

Calculations using SBBN models predict signatures that are likely to be observable in only in a few cases (i.e. the H, D, ^{4}He and ^{7}Li abundances). With so few parameters, interpretation of the signatures requires significant theoretical input. Only very tiny abundances are predicted for nuclides more massive than ^{7}Li. However, calculations based on IBBN models predict, over much of their parameter space, significant signals for heavier nuclides. Present day telescopes are approaching the sensitivity where discrimination between SBBN and IBBN may be feasible by looking for these heavier nuclides, with much of the remaining uncertainty being dominated by the uncertainty in the ^{8}Li(α,n)^{11}B reaction rate.

In the standard model, the triple alpha reaction dominates the synthesis of ^{12}C. According to IBBN models however, the main pathway to the production of ^{12}C is the nuclear reaction chain: ^{1}H(n,γ)^{2}H(n,γ)^{3}H(d,n)^{4}He(t,γ)^{7}Li(n,γ) ^{8}Li(α,n)^{11}B(n,γ)^{12}B($\beta\nu$)^{12}C. Due to the short half-life of ^{8}Li (840ms) and the reacting particles having the highest Coulomb barrier in this chain, the ^{8}Li(α,n)^{11}B reaction rate greatly influences the flow of material through this pathway. Although, this reaction has very little effect on the predicted ^{11}B abundance, most of the abundance of more massive nuclides, ^{12}C and heavier, are generated at the time when the ^{8}Li abundance is large, so that ^{8}Li(α,n)^{11}B is crucial for predicting their abundances. Thus it is important that its cross section be accurately measured in order to distinguish between the different predictions of the two models.

1.2 r-process Nucleosynthesis

The ^{8}Li(α,n)^{11}B reaction has recently been identified as also playing an important role in r-process nucleosynthesis occurring in the supernovae environment. In the region of a type IIa supernova between the nascent neutron star and the shock front, all nuclei are believed to have been reduced to protons and neutrons by the passage of the shock wave. They then reform mostly under nuclear statistical equilibrium and the nuclides so produced become the seed nuclei for the r-process. However, the critical step in this is the formation of ^{12}C and it is here that the ^{8}Li(α,n)^{11}B reaction can be important.

Recent network calculations[2,3] with an extended reaction network including all reactions involving light neutron rich nuclei indicated that, for models with short dynamic

timescales, the inclusion of the pathway that involves the ^{8}Li(α,n)^{11}B reaction changes the final heavy nuclei abundances significantly as compared to previous network calculations[4,5]. The formation of ^{12}C seed nuclei is inhibited by the need to bridge the mass 8 gap with the three body reaction $\alpha(\alpha n,\gamma)^{9}$Be. However, if sufficient ^{8}Li builds up in the r-process site for the reaction path, $\alpha(t,\gamma)^{7}$Li(n,γ)^{8}Li(α,n)^{11}B to proceed, then this pathway can have a significant effect on the ^{12}C abundance and consequently, on the abundance of r-process seed nuclei. Moreover, the required levels of ^{8}Li can be relatively small since this reaction pathway involves only two body reactions. Hence, improved measurements of the ^{8}Li(α,n) reaction will allow better estimates of reaction flow through these chains, influencing the final predicted abundances.

2 Previous Measurements

Several previous experiments have been undertaken to study this reaction. Paradellis *et al.*[6] performed a measurement of the inverse reaction ^{11}B(n,α)^{8}Li which provided an excitation function, covering a centre of mass energy range of 0.4 to 5 MeV, for the reaction to the ground state of ^{11}B. Measurements by Boyd *et al.*[7], covering an energy range of 1.5 to 6.2 MeV in the centre of mass, and Gu *et al.*[8], covering an energy range of 0.6 to 2.2 MeV, determined excitation functions for all states inclusively using a multiple-sampling ionisation chamber type detector. The discrepancy in cross section between the sets of direct and inverse reaction measurements was attributed to the population of excited states in ^{11}B.

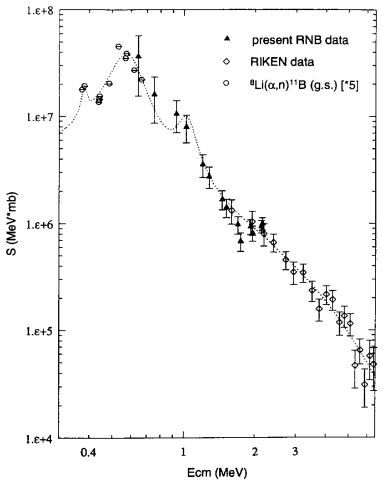

Fig. 1 S-factor figure taken from [8](see text).

Fig. 1 shows the S-factor figure taken from [8]. A broad resonance at approximately 0.6 MeV ($\Gamma \approx 200$ keV) can clearly be seen in the inverse reaction data (open circles) of Paradellis *et al.* However, an indirect study of this reaction via the reactions ^{9}Be(α,p)^{12}B and ^{11}B(d,p)^{12}B was performed by Mao *et al.*[9] and while several ^{12}B states in the astrophysically relevant energy range were observed, there was no evidence of this broad resonance. Consequently, a measurement which provides concrete evidence for the pres-

ence and parameters of this resonance is highly important since it will play a critical role at the astrophysically relevant temperatures. A discussion by Boyd *et al.*[10] of all available data, including indirect measurements, concluded that resonant contributions accounted for only half of the cross section at low energies and thus the direct process must also make a significant contribution. A more recent study by Mizoi et al.[11] which measured the cross section to ^{11}B states exclusively indicated a factor of two discrepancy, for the ratio of total cross section to ground state cross section, as determined from previous measurements. Moreover, the results of [7,8] and [11] all suffer from poor statistics. Fig. 2 is taken from [11] and shows the current data available on the total cross section (left) and astrophysical S-factor (right). Consequently, a measurement that determines total and partial cross sections for this reaction and provides clarification on the origins of this discrepancy is necessary.

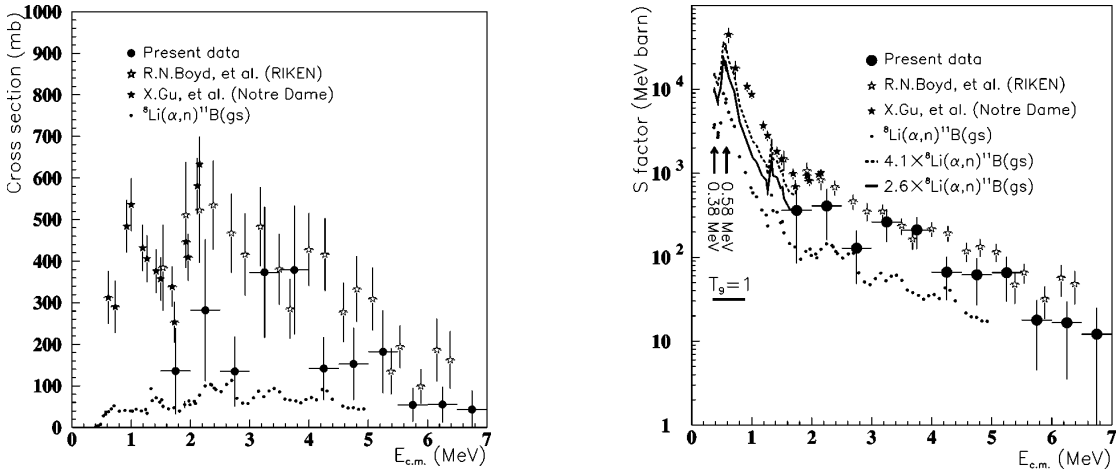

Fig. 2 Cross section (left) and S-factor (right) results to date, taken from [11](see text).

There has been a more recent attempt at the study of this reaction here at TRIUMF. The TOJA (Triumf Ohio State Japanese Affiliation) were granted beamtime for experiment E812[12]. The approach adopted for this study was based on the detection of the emitted neutrons. However, this method proved to be unsuccessful in this case due to prohibitively high backgrounds and insufficient beam intensity. Consequently, the current proposal has a different approach, namely the detection and measurement of the emitted ^{11}B particles and γ-rays.

3 Description of the Experiment

We propose to measure directly the cross section for the ^{8}Li(α,n)^{11}B reaction by tracking the recoiling ^{11}B in an ionisation chamber and by detecting, in coincidence, the γ-rays in those cases where excited states in ^{11}B were populated. We propose to measure the angular distributions for the population of each of the relevant states for centre of mass energies between 0.4 and 3.0 MeV. This will allow the determination of the partial and total cross sections at astrophysically relevant temperatures.

A new detector will be designed and built specifically for this measurement. The ion chamber will be cylindrically symmetric about the beam axis and will consist of a cylindrical central region bounded by a thin foil and surrounded by the active bulk of the detector (see Fig. 3). The central region contains helium and acts as the target. The thin foil bounding this region is aluminised and will act as the cathode of the ion chamber. The surrounding region contains isobutane as the detector gas. There will be a cylindrical Frisch grid surrounding the central region which will be positively biased compared to the cathode. Outside this grid, there will be circular anode rings positioned perpendicular to the beam axis to collect the signal. Each anode ring will be segmented into several strips. At either end of the central region, upstream and downstream of the target, the gas will be contained by foil windows. The chamber will be surrounded by a γ-detector array.

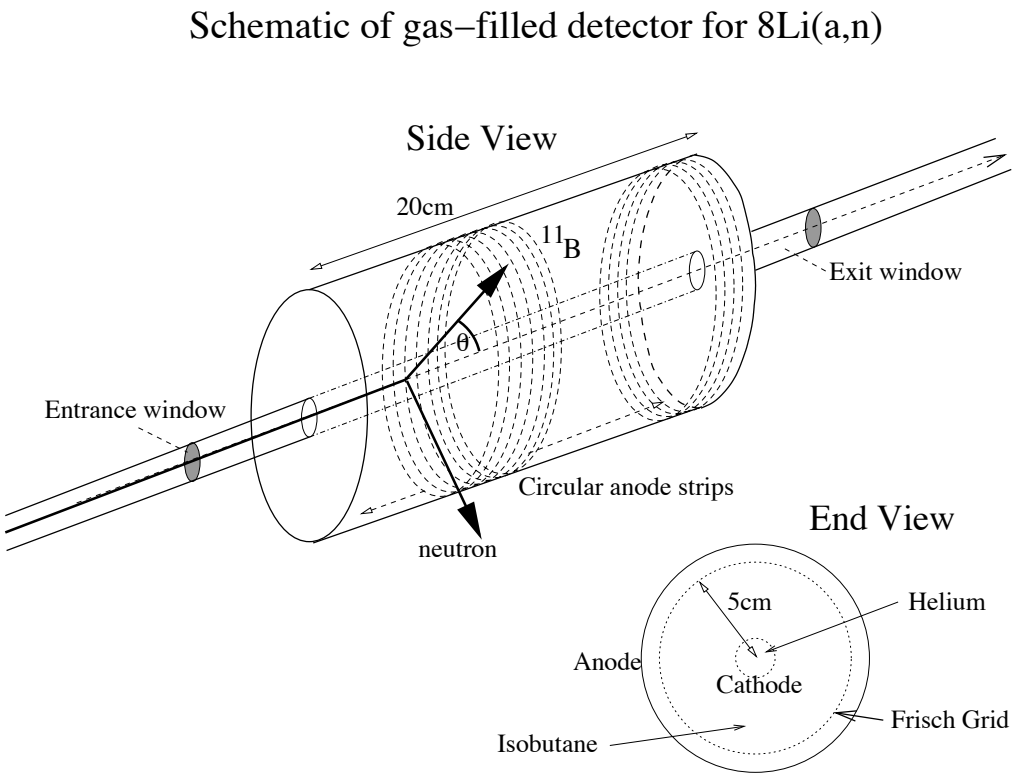

Fig. 3 Schematic view of the gas detector.

The ^{8}Li beam enters the ion chamber through the foil window. Interactions can occur along the length of the helium region and scattered particles and reaction products emitted at angles greater than approximately 2 degrees pass through the cathode foil and are tracked in the detector bulk. The beam itself passes out through the exit window and will be stopped at a distance from the detector. Since only scattered particles and reaction products are tracked in the detector, higher beam rates can be handled than in previous measurements where each beam particle was tracked. Here the rates will be dominated by elastic scattering. Assuming drift times of the order of μs, beam intensities up to 10^{7} pps can be handled without significant pileup.

As the particles traverse the detector gas, the resulting ionisation electrons are drifted to the anodes and collected. The current and position of the anodes allows identification of the particle from energy loss per cm and also reconstruction of the particle trajectory. From this, the point along the detector axis at which the reaction took place can be determined and the reaction energy calculated. The relative drift times of the electrons through the gas give the angle at which the particle was emitted, relative to the beam axis.

The beam energy as a function of gas pressure will be determined independently by direct measurement of the beam energy using a silicon detector. This data will be used together with SRIM simulations to determine the beam energy as a function of distance through the target, for each pressure.

Due to the inverse kinematics, the ^{11}B particles are forwardly focussed. The maximum ^{11}B emission angle varies from 23 deg. at E_{cm}=3. MeV to 64 deg. at E_{cm}=0.4 MeV. For reactions occuring in the first half of the target, the detector covers approximately 85 percent of the ^{11}B emission cone. For reactions further downstream, this angular coverage drops off. The exact geometrical efficiency of the ion chamber will be determined from Monte Carlo simulations. Fig. 4 shows the kinematics of scattered ^{8}Li and ^{11}B for a beam energy of 3.3 MeV. The energy losses in the windows have been taken into account.

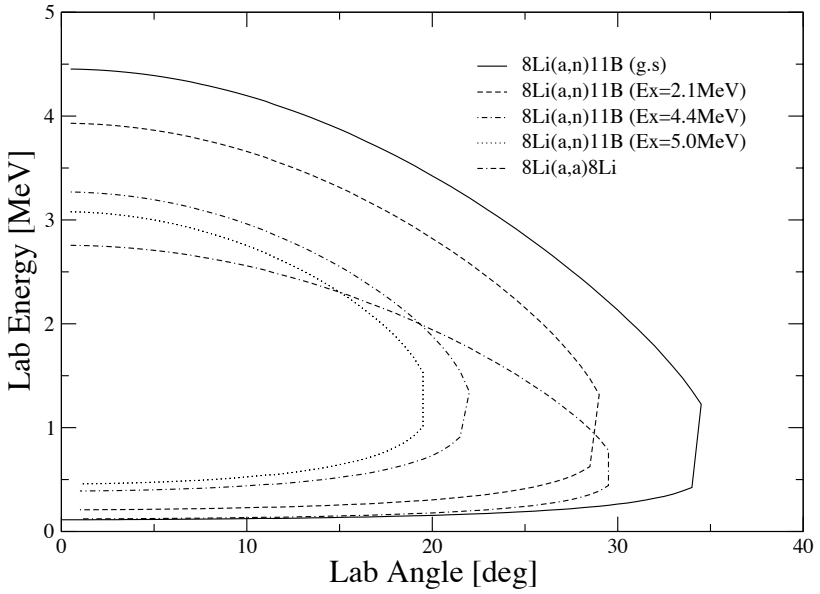

Fig. 4 Energy vs. angle of ^{11}B and elastically scattered ^{8}Li at E_{beam}=3.3 MeV.

The main source of background will be from elastic scattering. However, several features allow these events to be discriminated from real events. As can be seen from Fig. 5, the scattered α-particles and ^{8}Li have sufficiently different energy losses and can be differentiated from ^{11}B. Scattered ^{8}Li also have sufficiently different energies as compared

to ^{11}B populated in the ground state. Moreover, scattered α-particles and ^{8}Li will be in coincidence and for those ^{11}B populated in excited states, the prompt γ-rays provide another method for differentiating real and background events.

The ^{12}B from radiative α capture, a possible secondary source of background, will have very small emission angles and will majoratively be confined to the region bounded by the cathode. Since the radiative capture reaction has a higher Q-value than ^{8}Li(α,n)^{11}B, any ^{12}B stopped in the detector can be identified due to its higher energy. In any case, the cross section for this reaction will be smaller than that of the ^{8}Li(α,n)^{11}B reaction.

The entrance and exit windows, another common source of background, will be placed at distances away from the detector such that scattered particles from these windows will not enter the active region of the detector. A collimator may be placed after the entrance window based on results from the testing stage.

The entrance window will be mounted at the exit of a diagnostics box to be located just upstream of the ion chamber. This unit will contain collimators, a movable Faraday Cup and a 4 vane beam monitor to facilitate tuning of the beam through the ion chamber. This box will also contain a small silicon detector which will monitor the beam intensity during a run from backscattering off the entrance window.

The beam will pass through the exit window and will be stopped in a long Faraday cup at a distance such that radiation from the decay of the beam particles will not interfere with the detectors. The current reading from the Faraday Cup will be used for normalisation.

The γ-ray detection system will consist of an array of 30 BGO detectors. These detectors will be mounted on a custom made support structure and will surround the cylindrical surface of the ion chamber. The main source of background will arise from the decay of the beam particles. Other sources include γ-rays from the radiative capture reaction and the ambient room background. However, the background can be significantly reduced by first requiring an event in the ion chamber before accepting a BGO signal.

In addition, to the ^{8}Li(α,n)^{11}B cross section data, information on the elastic scattering channel should also be obtained allowing R-matrix calculations to be performed.

4 Detectors and Electronics

4.1 Ionisation Chamber

The ionisation chamber will be optimised for tracking and identifying the particles produced during a measurement of the ^{8}Li(α,n)^{11}B reaction.

The detector will be designed to run in two configurations. The standard configuration is as described briefly above with an aluminised thin window separating the helium target gas and the isobutane in the active region. The gas handling system will maintain a constant and equal pressure in both regions to minimise strain on the window. Gas pressures are anticipated to be in the region of 15 to 50 mbar. This corresponds to an energy loss of 10-20 keV/cm for the incident ^{8}Li. This pressure will be matched to the beam energy so that the ^{11}B will be stopped within the detector and there is sufficient

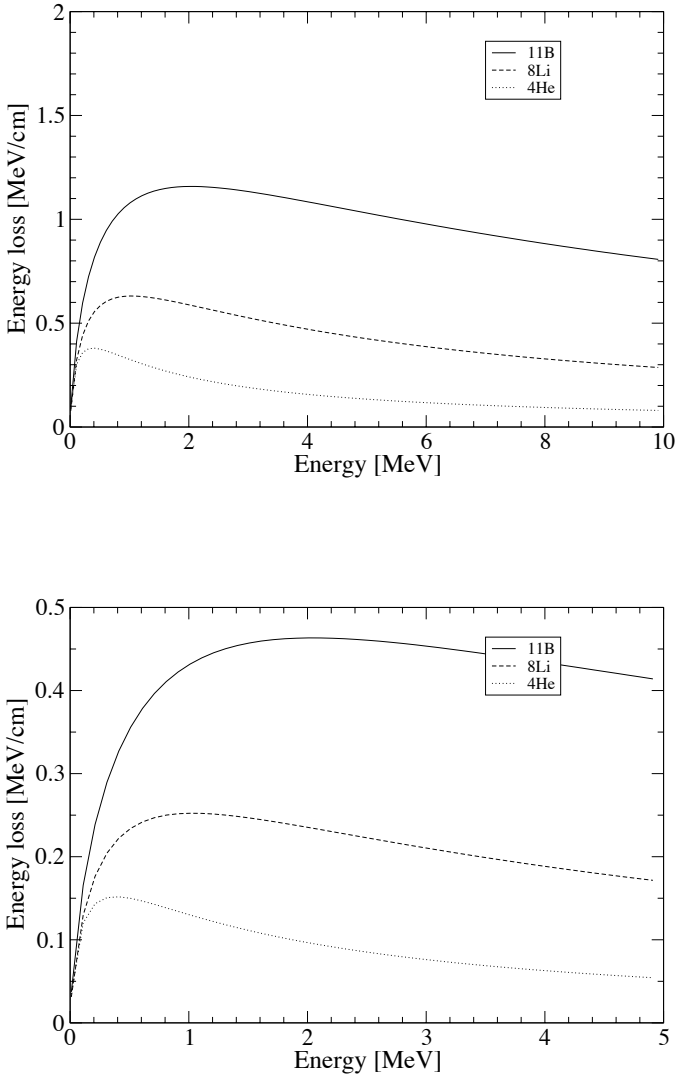

Fig. 5 Energy loss as a function of energy for selected ions in 50 mbar (top) and 20 mbar (bottom) of isobutane

energy loss per cm for particle identification. Optimum pressures and voltages will be determined during the testing stage.

The cylindrical cathode will be attached at either end to metal rings which can then be mounted on flanges on the inside wall of the vacuum chamber. The cylindrical Frisch grid will also be supported at either end by attachments to the inside wall of the chamber. The anode strips will be etched on G10 (material commonly used for printed circuit boards, consisting of copper over fiberglass laminate) which can be shaped into a cylinder and likewise mounted on the chamber wall. There will be approximately nineteen 1cm wide anode strips. Feedthroughs for signal and voltage cables will be mounted on either end of the chamber.

The pumping system will be mounted on the beamline at either side of the chamber, just upstream of the exit window and downstream of the entrance window. Gauges will monitor the pressure in both regions of the detector and adjust gas flow accordingly. The isobutane gas handling system will be on one end of the chamber while the helium gas handling system will integrate with the pumping system.

At the lowest beam energies, however, the aluminised window separating the gases will be removed and replaced with thin wires running longitudinally to act as the cathode. The entire detector will be filled with helium gas with a small mixture of isobutane. This eliminates the energy loss in the internal window, allowing smaller particle energies to be measured.

4.2 γ-detector Array

We propose to use the DRAGON BGO for gamma detection. The thirty BGO detectors will be mounted surrounding the chamber containing the ion chamber. The support for the BGO detectors will be designed to optimise geometric coverage. The BGO efficiencies will be determined from Monte Carlo simulations and source measurements. Also, the dependence of the detection efficiency on the position of the interaction in the target will be determined from stable beam (α, γ) resonance measurements. Resonances with known energies and strengths can be populated and the yield, as function of position in the target, scanned by changing the beam energy.

4.3 Electronics

The current TUDA amplifiers and the VME DAQ should be suitable for this application. New preamplifiers will need to be purchased. Energy and timing signals with respect to the RF will be acquired for each channel.

For the BGO-array, the related electronics from the DRAGON setup will be integrated with the TUDA data acquisition.

5 Readiness

This experiment requires the design and construction of a customised ionisation chamber. This includes the vacuum chamber, gas handling system, beam diagnostics box and necessary electronics. Also requiring fabrication are a beam diagnosis chamber, to be located upstream of the ion chamber, and a support structure for the BGO detectors. We expect to utilise the TUDA VME data acquisition system which is due to be installed and tested later this year. The BGO array with necessary electronics will be moved from DRAGON to the TUDA beamline as and when necessary. We have applied to NSERC for funding for the ionisation chamber and assuming funding is granted we expect to have construction and testing complete by fall 2004.

6 Beam Time required

The previous exclusive measurement reported a total cross section to all states in ^{11}B of 140 mb at a centre of mass energy of 1.8 MeV. Assuming this cross section, a target thickness of 10^{19} cm^{-2} and a beam intensity of 10^7 pps gives a count rate of the order of 5 real events every second, taking into account efficiencies. For an average of 3000 counts per state, each energy measurement is projected to take 1.5 hours. We propose to cover the centre of mass energy range in steps in 50 keV, i.e. 54 energy settings, covering the excitation function for centre of mass energies from 0.4 to 3 MeV. Therefore, taking into account the time necessary for energy changes, we request 20 shifts of ^{8}Li beam.

In order to determine the performance of the proposed experimental setup, we intend to use the ^{9}Be(α,n)^{12}C reaction which has well known cross sections and angular distributions. This reaction has a similar Q-value and kinematics to the reaction under study. Therefore, we request 20 shifts of stable ^{9}Be beam for testing the system and for calibration purposes. In addition, we request 10 shifts of stable ^{7}Li beam in order to determine our experimental resolutions.

7 Data Analysis

The DAQ will be triggered by an event in any anode strip and the acquisition gate will be closed by a subsequent RF pulse. Only BGO signals arriving within this time gate will be acquired, i.e. only γ rays in coincidence with a heavy ion will be accepted. The expected rates are such that all events in the ion chamber which occur within the time window defined by the RF will be acquired without significant dead time losses. On line analysis will be used to monitor the status of the detectors and the beam. In addition, using the data from the stable beam runs, attempts will be made to include particle identification in the on-line analysis.

References

1. N. Hata et al., Phys. Rev. Lett. **75**, 3977 (1995)
2. M. Terasawa et al., Astro. J. **562**, 470 (2001)
3. T. Kajino et al., Nucl. Phys. **704**, 165c (2002)
4. B. S. Meyer et al., Astro. J. **399**, 656 (1992)
5. S. Woosley et al., Astro. J. **433**, 229 (1994)
6. T. Paradellis et al., Z. Phys. **A 377**, 211 (1990)
7. R. Boyd et al., Phys. Rev. Lett. **68**, 1283 (1992)
8. X. Gu et al., Phys. Lett. **B. 343**, 31 (1995)
9. Z.Q. Mao et al., Nucl. Phys. **A 567**, 111 (1994)
10. R. Boyd et al., Comm. Nucl. Part. Phys. **22** 47 (1996)
11. Y Mizoi et al., Phys. Rev. **C 62**, 065801 (2000)
12. TRIUMF Research Proposal E812, Spokesperson Prof. D. Boyd

Include publications in refereed journal over at least the previous 5 years.

1. *Strong resonances in elastic scattering of radioactive ^{21}Na on protons*
   C. Ruiz, F. Sarazin, L. Buchmann, T. Davinson, R.E. Azuma, A.A. Chan, B. Fulton, D. Groombridge, L. Ling, A. Murphy, J. Pearson, I. Roberts, A. Robinson, A.C. Shotter, P. Walden, and P.J. Woods.
   Phys. Rev. C **65** 042801, (2002)

2. *The (π^+, pd) and (π^+, dd) Reactions on Light Nuclei at 100 and 165 MeV Incident Pion Energies*
   G.M. Huber, G.J. Lolos, Z. Papandreou, J. Hovdebo, S.I.H. Naqvi, D.F. Ottewell, P.L. Walden, G. Jones, and X. Aslanoglou.
   Nucl. Phys. A **705** 367-395 (2002)

3. *Apparatus for a measurement of charge symmetry breaking in $np \to d\pi^0$*
   D.A. Hutcheon, R.A. Abegg, E.G. Auld, R.M. Churchman, C.A. Davis, R.M. Finlay, P.W. Green, L.G. Greeniaus, R. Henderson, D.V. Jordan, W. Kellner, E. Korkmaz, A.K. Opper, G.V. O'Rielly, T.A. Porcelli, S.D. Reitzner, G. Sheffer, P.L. Walden, and S. Yen
   Nucl. Instr. and Meth. A **459** 448 (2001)

4. *Inclusive measurements of the $pp \to pn\pi^+$ reaction at 420 and 500 MeV.*
   R.G. Pleydon, W.R. Falk, M. Benjamintz, S.Yen, P.L. Walden, R. Abegg, D. Hutcheon, C.A. Miller, M. Hartig, K. Hicks, G.V. O'Rielly, R. Shyam
   Phys. Rev. C. **59** 3208-3223 (1999)

5. *Analyzing Powers and Partial Wave Decomposition of $pn \to pp(1_0^S)\pi^-$ at Low Energies.*
   H. Hahn, F. A. Duncan, J. Aclander, D. Ashery, E. G. Auld, D. R. Gill, D. A. Hutcheon, G. Jones, E. Korkmaz, S. Maytal-Beck, M. A. Moinester, J. A. Niskanen, D. Ottewell, A. Rahav, S. Ram, M. Sevior, P. L. Walden, and R. Weiss
   Phys. Rev. Lett. **82** 2258-2261 (1999).

6. *Gamow-Teller strength in (n, p) charge exchange on ^{31}P*
   R. M. Sedlar, T. P. Gorringe, W. P. Alford, D. A. Beatty, J. Campbell, H. T. Fortune, P. Hui, D. A. Hutcheon, R. B. Ivie, K. P. Jackson, A. G. Ling, Z. Mao, M. G. McKinzie, B. Siebels, D. A. Smith, P. Walden, and S. Yen
   Phys. Rev. C. **59** 789-795 (1999)

7. *Optical Design and Performance of the SASP Spectrometer at TRIUMF*
   P.L. Walden, T.G. Walton, C.A. Miller, S. Yen, R. Abegg, E.G. Auld, J. Campbell, J. Chakhalyan, R. Churchman, F. Duncan, W. Falk, D. Frekers, A. Green, P.E.W. Green, M. Hartig, O. Hausser, C. Haddock, K. Hicks, D. Hutcheon, G. Jones, Y. Ke, E.J. Korkmaz, N. Khan, A. Ling, D.E. Lobb, S.I.H. Naqvi, W.C. Olsen, A. Opper, A. Otter, M. Punysena, P. Reeve, Z. Zhao
   Nucl. Instr. and Meth. A **421** 142-162 (1999)

8. *Investigation of the $^{12}C(\vec{p}, d\pi^+)^{11}B$ reaction in the quasifree region*
   M. Benjamintz, W. R. Falk, J. R. Campbell, A. Green, P. G. Roos, P. L. Walden, S. Yen, A. G. Ling, E. G. Auld, E. Korkmaz, M. A. Punyasena
   Phys. Rev. C. **58** 964-980 (1998)

9. *Differential Cross Section of the $pn \rightarrow pp(^1S_0)\pi^-$ Reaction Extracted from $pd \rightarrow ppp\pi^-$*
   F. Duncan, H. Hahn, C. Aclander, D. Ashery, E. G. Auld, D. R. Gill, D. A. Hutcheon, G. Jones, E. Korkmaz, S. Maytal-Beck, M. A. Moinester, J. A. Niskanen, D. Ottewell, A. Rahav, S. Ram,M. Sevior, P. L. Walden, and R. Weiss
   Phys. Rev. Lett. **80** 4390-4393 (1998).

10. *Multinucleon Contributions to the $^{12}C(\pi^+, pp)$ Reaction at 100 and 165 MeV Incident Pion Energies.*
    G.M. Huber, G.J. Lolos, Z. Papandreou, J.C. Cormier, E.L. Mathie, S.I.H. Naqvi, D.F. Ottewell, P.L. Walden, G. Jones, R.P. Trelle, X. Aslanoglou, and J.L. Visschers.
    Nucl. Phys. **A624** 623-654 (1997).

11. *Spin-Transfer Measurements of the $\pi\vec{d} \rightarrow \vec{p}p$ Reaction at Energies Spanning the Δ Resonance.*
    A. Feltham, G. Jones, R. Olszewski, M. Pavan, M. Sevior, R.P. Trelle, P. Weber, G.J. Lolos, E.L. Mathie, Z. Papandreou, R. Rui, D. Gill, D. Healey, D. Ottewell, G. Sheffer, G.R. Smith, V. Sossi, G. Wait, and P. Walden.
    Phys. Rev. C. **55** 19-41 (1997)